Citation: Vicente, Asier, Artzai Picon, Jose Antonio Arteche, Miguel Linares, Arturo Velasco, and Jose Angel Sainz. “Magnetic Field-Based Arc Stability Sensor for Electric Arc Furnaces.” Measurement 151 (February 2020): 107134. doi:10.1016/j.measurement.2019.107134.

DOI: https://doi.org/10.1016/j.measurement.2019.107134

Magnetic field-based arc stability sensor for electric arc furnaces.

Asier Vicente-Rojo[a*], Artzai Picon[b], Jose Antonio Arteche[b], Miguel Linares[b], Arturo Velasco[a], Jose Ángel Sainz[a]

[a] Arcelor Mittal Research Centre, Sestao,Spain.
[b] Computer Vision, TECNALIA, Parque Tecnológico de Bizkaia, C/ Geldo. Edificio 700, E-48160 Derio, Bizkaia, Spain
* Corresponding Author: e-mail: asier.vicente@arcelormittal.com).

***Abstract*—**

During the last decades the strategy to define the optimal Electric Arc Furnaces (EAF) electrical operational parameters has been constantly evolving. Foaming slag practice is currently used to allow high power factors that ensures higher energy efficiency. However, this performance depends on strict electric arc stability control. Control strategies for these are normally defined for alternating current furnaces (AC EAF) and are based on intrusive and highly expensive systems. In this work we analyze the variation of the magnetic field vector around the direct current EAF (DC EAF) and its relationship with arc stability. We propose a cheap stability control system with no installation or integration requirements and thus, easily implementable to both AC and DC EAFs. To this end we have built a non-intrusive and low-cost 3-axis Hall-effect sensor that can be mounted neighboring the furnace's electrical bars. The sensor allows acquiring the magnetic field magnitude and orientation that provides a newly defined arc stability factor metric. This proposed Arc Stability Index has been compared with three different alternative well established and more expensive measurement methodologies obtaining with similar results. The proposed index serves as a closed loop signal to the electrical regulation for controlling the arc voltage, ensuring the most convenient arc length that guaranties non-instabilities. The new system was developed and industrially validated at two different DC EAF's in ArcelorMittal demonstrating an improvement of 6.7 kWh per Liquid steel ton during the evaluated period and a time reduction of 1.1 minutes per heat over the current standard procedure. Additional validation tests were also carried out also in ArcelorMittal AC EAF proving the capability of this technology for both AC and DC of furnaces.

***Index Terms*—Electric Arc Furnace, Arc Stability, Magnetic Field, Hall Effect, Electrical Efficiency**

I. INTRODUCTION

Modern metallurgic processes require highly optimized to compete in terms of quality and energy savings. In modern steel production, steel can be obtained by two different processes: Iron-making route (from iron ore) and electrical steelmaking route (from scrap metal). Both processes follow two subsequent stages of oxidizing and reducing the steel to adequate the component to the steel grade requirements. In both cases, the main objectives of metallurgic processes is to produce a product that complies with the final products specifications. These requirements highly depend on the final composition of the steel. Other metallurgic processes also make use of oxidizing-reducing subsequent stages to obtain materials with the appropriate quality requirements such as silicon manufacturing[1][2]

Given the flexibility required to quickly adapt the production from one strategy to another according steel market demand variations, electric steelmaking process presents some important advantages over iron making route such as flexibility, higher productivity and higher process yield. However, one of the main drawbacks is the low energy efficiency of the process, since approximately 40% of the total energy consumed by the EAF represents energy losses [3].The usual energy balance for EAF proves that there is significant room for improvement when balancing productivity requirements with efficient energy input strategies [4]. The awareness by steelmaker on this concept has motivated continuous development of new process monitoring [5][6][7], control [8][9] and optimization methods [10][11][12] aiming to reduce production costs, while maintaining targeted steel quality (steel grade), facility productivity and meeting environmental standards (carbon emissions).

The electrical energy input factor has been thoroughly analyzed as the most determinant for the optimal EAF electrical operational control. Control strategy has evolved considerably [17]. In the 1970´s increased

powering emphasized the minimization of refractory erosion and, consequently, low levels of voltage, reactance and power factor were recommended. After the arrival of the water-cooled panels it was possible to operate with higher voltages during a great period of the melting period and a significant reduction in electrode consumption was achieved. Later, in the 1980´s, the development of the foamy slag[18] allows a new voltage increase, also during the flat bath period, leading to further power increment and electrode consumption reduction. Presently, it was confirmed that good foamy slags allow the operation with very high-power factors at the last stage of melting, without arc instability [21].

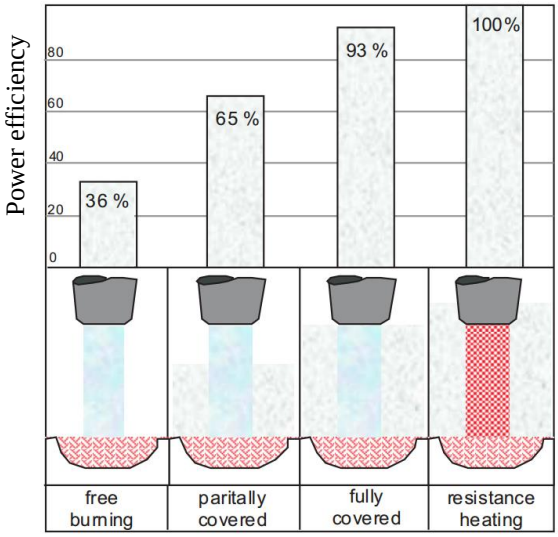

Fig. 1. Influence of foaming slag to the efficiency of power input [18]

Fig. 1 depicts the influence of foaming performance of slag on the energy input efficiency. However, it is not always possible to control the chemical aspects of the process, and it is often necessary to act over the electrical parameters to ensure that the process is stable. Currently there are several methodologies to estimate the appropriate level of voltage that yields to a minimization of arc instabilities while maintaining an optimal productivity. As over 85% of electric steel is made in AC EAFs and only 15% is made in DC EAF[16], most of the efforts to increase the arc efficiency have been conducted on AC technologies. The most extended method consists of analyzing harmonics generated in the electrical supply by the arcs as a foaming slag monitor by mean of Rogowski coils [19]. These approaches had been normally used to predict and correct the effect of the power network disturbances caused by AC EAF operations [13][14][15][20][21] and for arc instability estimation [23] and have been successfully built and fitted to the electrode power cables [24], as a better foaming slag leads to a more stable arc and fewer harmonics. However, they cannot be used for DC EAF measurement. Other methodologies include the analysis of high-frequency acoustic signal processing [25] or measurement of the Optical Emission produced by the electrode arcing [26] but these control methodologies require technical installation in EAF and, so that can be consider as intrusive methods.

On the other hand, it is common knowledge that the strong magnetic fields on EAF proximities present high variation during arc instabilities and its online measurement can be considered a good indirect measurement of the arc stability. Although there are numerous approaches for magnetic field measurements [28]. Hall effect-based sensors have proven successful for metrology [27] fault detection on power systems [29] , broken rotor bars diagnosis in large induction machines[30] and numerous applications for non-destructive essays [31] even for highly sensitive scientific applications with a very low cost [32].

The demonstration that a low-cost Hall effect-based sensor can be used for indirect measurement of the stability arc in an accurate manner will reduce the cost for implementing arc stability control methods which are expensive and intrusive currently requiring redesigning and technical electrical installation. This is of

great importance specially for already existing EAF furnaces that can benefit from current sensor.

Based on these premises, this work validates a new low-cost and non-intrusive sensor that, measures the magnetic field magnitude and orientation in the furnace's proximities and analyses the acquired signal providing an arc stability factor metric (*Arc Stability Index*). This Arc Stability Index has been validated against other existing measurement alternatives (acoustic sensor, slag, bath computer vision-based inspection, expensive commercial fault detection system) with better or similar performance. The sensor has been integrated on existing DC and AC EAFs demonstrating a power reduction of 6.7 kWh per Liquid steel ton during the evaluated period and a time reduction of 1.1 minutes per heat.

The paper is organized as follows. In Section II, we provide the theoretical concepts with regards to magnetic fields and Hall effect sensors. Sections III describes the design of a 3D Hall sensor based on three different 1D Hall sensor components. Section IV defines mathematically the proposed *Arc Stability Index* This *Arc Stability Index* is compared against the response of three different alternative measurement techniques (acoustic sensor, slag, bath computer vision-based inspection, expensive commercial fault detection system) where high correlation is obtained. Section VI proposes a control algorithm based on the Arc Stability Index and validates the energy savings of the proposed sensor and Arc-Stability Index when used to regulate two DC and AC EAFs on real production settings. Finally, section VII concluding remarks are provided.

II. Magnetic Field Measurement

Let I_{arc} be the current flowing through the conductor that generates the arc in the EAF, D the distance from the measurement place and μ_o, the magnetic permeability of free space, the magnetic field generated on a point in the space is then defined by equation 1:

$$B = \frac{\mu_o \cdot I_{arc}}{2\pi D} \qquad (1)$$

Magnetic field measurement ranges from simply sensing the presence or change in the field to the precise measurements of a magnetic field's scalar and vector properties. One of the methodologies used for magnetic field relies on the Hall effect. The Hall-effect sensor is based on the discovery of Edwin H. Hall in 1897. The Hall effect is a consequence of the Lorentz force law, which states that a moving charge (***q***) in an electric field (**E**), when acted upon by a magnetic induction field (***B***), will experience a force (***F***) that is at right angles to the field vector and the velocity vector (***v***) of the charge as expressed by the equation 2:

$$\vec{F} = -q(\vec{E} + \vec{v}x\overrightarrow{B}) \qquad (2)$$

This principle has been applied in the development of Hall-effect sensors which are activated by an external magnetic field ***B***. If a Hall sensor powered by a voltage ***E*** is placed on a magnetic field, a voltage V_{out} proportional to the product between the powering current and the intensity of the normal component to the magnetic field ***B*** with respect to the sensor appears.

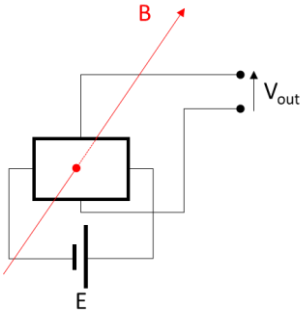

Fig. 2. Hall Sensor response

In this work we have selected a sensor (A1302) with a high magnetic sensitivity which provides a voltage output that is proportional to the incident magnetic field perpendicular to the sensor orientation according to equation 3:

$$V_{out} = V_{outQ} + Sens\frac{B_z}{1000} \quad (3)$$

Where V_{out} is the voltage output, V_{outQ} is the voltage in the quiescent state (no significant magnetic field: B = 0), *Sens* is the magnetic sensitivity (2.5 mV/G in our case) and B_z is the Z axis component of the incident magnetic field in Gauss considering the sensor mounted on the X-Y plane. This sensor is capable of measuring and tracking the changes over the Z axis projection of the magnetic field.

III. 3D Magnetic Field Sensor Development

Although 1D Hall-effect based sensor has already proven their capabilities for fault detection on AC current measurements [34], a single Hall sensor is only able to detect variations on the projection of the magnetic field which is normal to the sensor surface. In the case of EAF, the high variability of the magnetic field direction during the different steel casting stages makes the use of single 1D hall sensor unreliable to detect changes on the magnitude of the magnetic field. Since the electric conductors of the furnace to the electrodes are not straight rigid elements, near the furnace the direction at which the magnitude of the magnetic field will be maximum is unknown and presents variable orientation which precludes the use of common Hall sensors.

To overcome this limitation, a low-cost 3D Hall-effect sensor have been designed: Three different 1D hall sensors based on the A1302 integrated circuit have been placed on the planes X0Y, X0Z and Y0Z, each of them, capable of detecting the $\boldsymbol{B_x}$, $\boldsymbol{B_y}$ and $\boldsymbol{B_z}$ components of the magnetic field. These three sensors are built into a plastic box to create an industrial sensor and installed in front of the current conductors, as shown in figure 3.

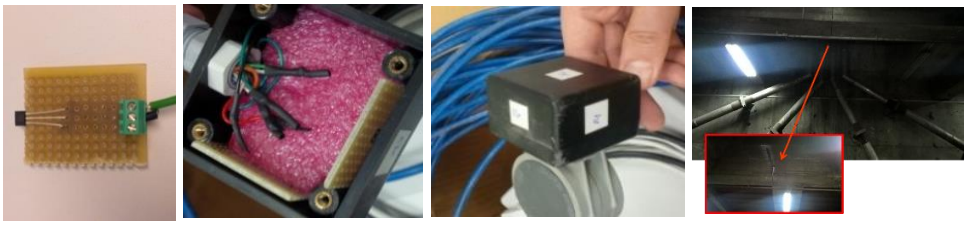

Fig. 3. Individual Hall sensor (Left), 3D Hall sensor and integrated sensor (Middle) and industrial installation (Right)

The developed sensor is directly mounted near the furnace's electrical bars capturing the magnetic field magnitude and 3D orientation of the magnetic field. Magnetic field information is continuously acquired by a NI 6211 acquisition card with 16bit capabilities at an acquisition rate of 1000HZ. These signals are transmitted to a Signal processor module that analyzes their spectral (frequency) properties and generates the Arc Stability Index that estimates the degree of stability on the electric arc. This index, which will be detailed on the next section, is used for power regulation on the EAF furnace to avoid arc instabilities during the steel casting process. Figure 4 describes the whole process.

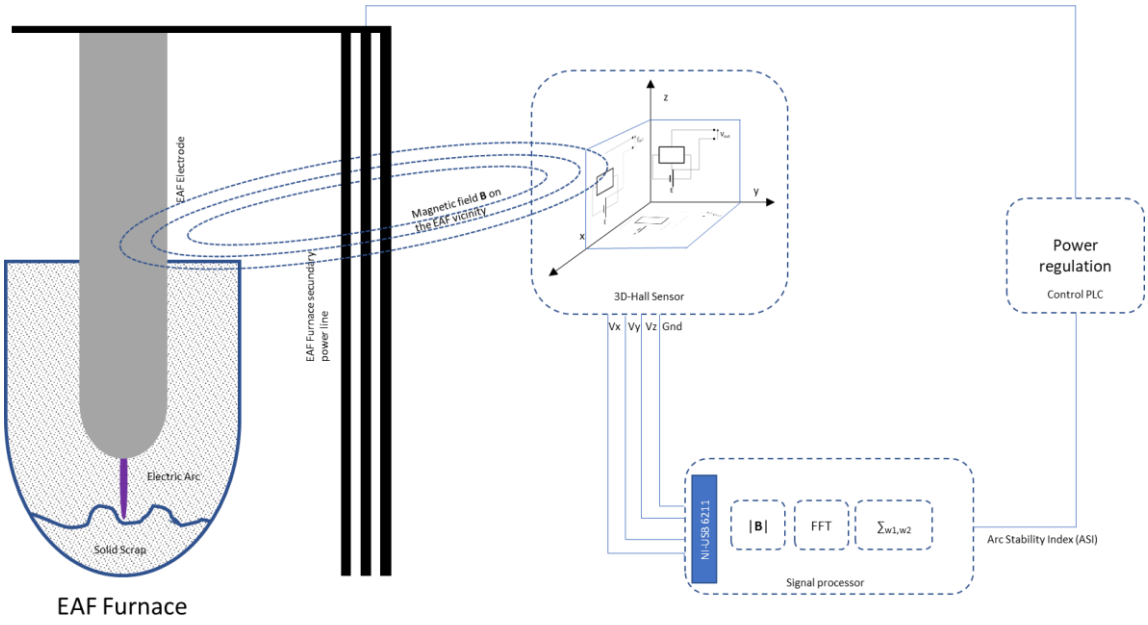

Fig. 4. Full concept diagram: EAF furnace with secondary power line. The proposed 3D Hall-Effect sensor is used to measure the three cartesian components of the magnetic field. These signals are continuously transmitted to the Signal processor that analyzes their spectral (frequency) properties and generates the Arc Stability Index. This Index is used for power regulation on the EAF furnace.

IV. Defining an Arc Stability Index Measurement

Common Arc Stability estimation approaches on AC EAFs are based on the use of Rogowski coils to predict and correct the effect of the power network disturbances caused by AC EAF operations in the electrode power cables [24], as a better foaming slag leads to a more stable arc and fewer harmonics. However, this approach cannot be used for DC furnaces. Based on the assumption that stable arc will present fewer harmonics also on the variation of the EAF magnetic field, we performed an initial acquisition of 12 sample casts and stored the variations of the magnetic field. Each cast was analyzed by an expert and temporally correlated with three different stability analysis methods: acoustic correlation, commercial intrusive stability control system and visual inspection. Based on this analysis, the acquired data was labeled as stable or unstable arc.

In order to analyse the harmonics of the temporal magnetic field signal, we generated a complete spectrogram of the magnetic field as a function of time and frequency that can depict the presence of harmonics along time. This is performed by calculating the Hanning windowed Fourier transform for each two second frame along the acquired temporal signal as seen in equation (4) where f(t) is the acquired signal, w is the Hanning window of length 2 seconds centered at time τ and τ, ω are the targeted time and frequency respectively of the windowed Fourier transform.

$$F(\tau,\omega) = \mathrm{wFFT}\{\mathrm{f(t)}, w\}(\tau,\omega) = \sum_{n=-\infty}^{\infty} \mathrm{f(t)} \cdot w\{t-\tau\} e^{-i\omega t} \tag{4}$$

Applying (4) to the magnitude of the magnetic field $\left\|\vec{\mathrm{B}}(\mathrm{t})\right\|$ we obtain the spectrogram $\mathrm{X}(\tau,\omega)$:

$$\mathrm{X}(\tau,\omega) = \mathrm{wFFT}\{\left\|\vec{\mathrm{B}}(\mathrm{t})\right\|, w\}(\tau,\omega) = \sum_{n=-\infty}^{\infty} \left\|\vec{\mathrm{B}}(\mathrm{t})\right\| \cdot w\{t-\tau\} e^{-i\omega t} \tag{5}$$

The calculated spectrogram $X(\tau, \omega)$ of the acquired cast was analysed. Figure 5 shows that regions labelled as unstable by the expert present higher dispersion on the vicinity of the frequencies that are natural multiple values of the frequency of the rectifiers (in the case of DC) or the power network (for AC). This can be appreciated in figure 5 where unstable regions present higher dispersion on the vicinities of 100Hz, 300Hz and 400Hz. Our hypothesis is that stable regions present signal on the Harmonic multiple frequencies while unstable regions present a dispersion on the frequential distribution of the signal.

Based on this appreciation, we design the Arc Stability Index (ASI) estimator as the dispersion on the frequential signal on the vicinity of a Harmonic band. We select 100Hz as central band as it has much lower signal noise ratio than the other bands. The Arc Stability Index is then calculated as the sum of the energy of the signal over the wavelengths on the vicinity of 100Hz that has been dispersed from this central frequency. ASI is described by equation (5) as the sum of the energy between ω_0 and ω_1 and the sum of the energy between ω_2 and ω_3.These values were empirically set to: $\omega_0 = 102Hz$, $\omega_1 = 120$Hz, $\omega_2 = 80Hz$, $\omega_3 = 98$Hz .

$$\mathrm{ASI}(\tau) = \sqrt{\sum_{\omega=\omega_0}^{\omega=\omega_1} X(\tau,\omega)^2 + \sum_{\omega=\omega_2}^{\omega=\omega_3} X(\tau,\omega)^2} \qquad (5)$$

Figure 5 depicts the acquired magnetic field signal $\|\vec{B}(\tau)\|$, where the stable and unstable regions are seen. The calculated spectrogram $X(\tau, \omega)$ and the proposed Arc Stability Index estimator based on equation (5).

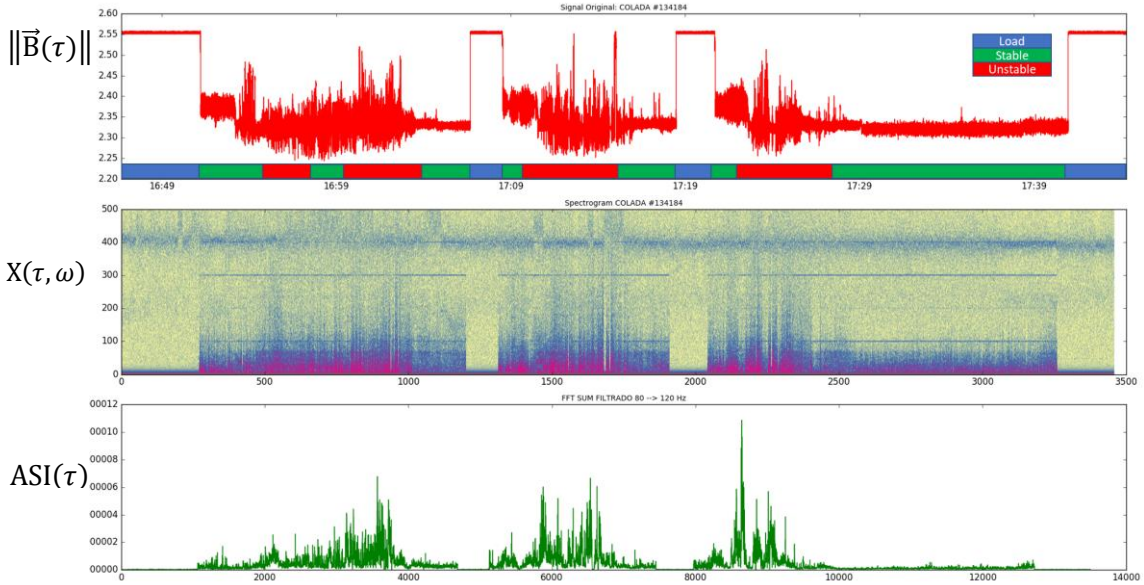

Fig. 5. Stability factor calculation. Top) Raw signal, Middle) Spectrogram, Bottom) Calculated stability index

.

This algorithm has been implemented on a .NET C# control application where NI 6211 acquisition card was used for data acquisition and communications with control PLC.

V. Industrial Validation of the Arc Stability Index

In this section we compare the proposed *Arc Stability Index* response with three different methods:

- Acoustic correlation.
- Comparative analysis against a validated expensive commercial sensor.
- Correlation with the visual analysis of the slag foam appearance by experts.

This analysis serves to correlate the arc stability estimation of the sensor with already stablished practices and methods.

A. *Acoustic Correlation*

The melting process in the electric arc furnace is closely linked to the noise level emitted by the furnace[25]. This is so to the extent that there are various commercial solutions based on noise analysis for estimating the slag foaming performance of the furnace. Although Acoustic correlation is a method with low intrusiveness, it is prone to low specificity and interferences from other EAFs. Using this principle, a sound meter was installed in front of an ArcelorMittal DC EAF. The objectives of this validation test were to confirm the direct relationship between magnetic field variation and noise evolution during non-stable phases, and to establish the instability threshold based on the analysis the sound meter data [25] when the furnace's operator decides to manually reduce the input power level.

Information from 34 different heats of approximately 60 minutes each were collected and sampled at 2000Hz. Simultaneously an Integrated sound level meter class 1 brand Brüel & Kjaer model 2270, together with acoustic calibrator RION Model NC-74 (class 1 according to IEC 60942) was installed at a DC Electric Arc Furnace in one ArcelorMittal steel plant and sound decibels were recorded.

Fig. 6 depicts three different casts where the blue line represents the stability factor and the brown one the decibels gathered by the sound meter. This demonstrates the strong correlation of our arc stability index and the acoustic signal processing methods.

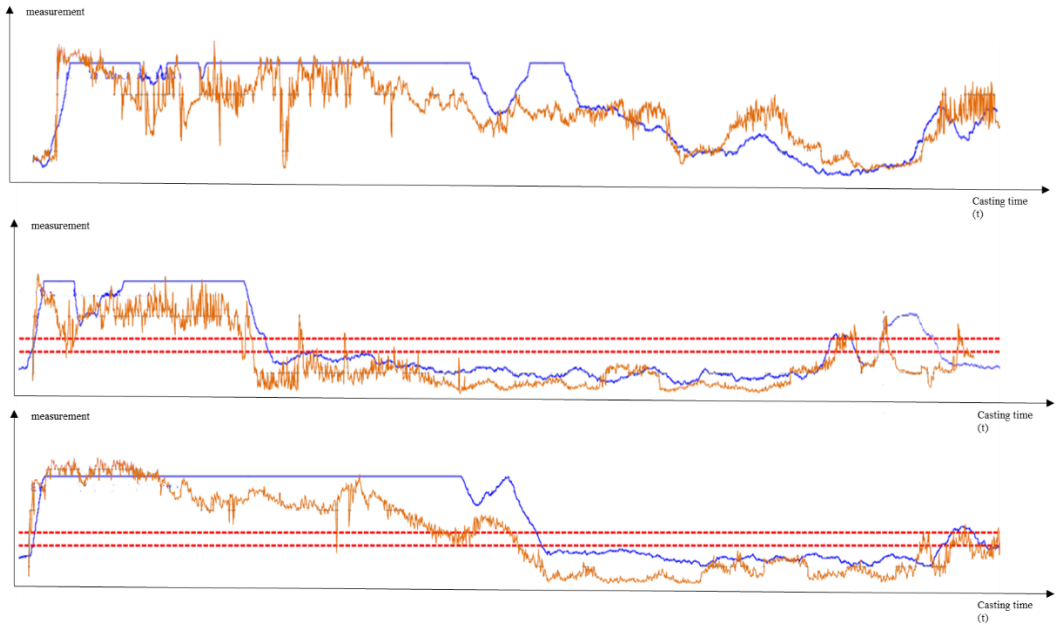

Fig. 6. Comparative analysis between Arc stability data and sound meter data in three different casts. Brown: Acoustic sensor (dB), Blue: Arc Stability index

B. *Commercial Stability Control System*

Prior to the definitive installation of the sensor in the selected furnace, the sensor for controlling instabilities was installed in one ArcelorMittal's DC EAF provided with a well-known electrical regulation system, which includes an arc stability control system. The objective of this preliminary validation phase was to demonstrate that the output signal, after the proposed processing methodology, had high correlation with the output of the commercial stability control system installed in the aforementioned furnace.

During this validation period, the heats produced during one production day were analyzed. For each of the analysis we recorded the arc stability values provided by the new proposed sensor and compared with stability index provided by the SMARTARC system by AMIGE available in the furnace, which performs

the stability analysis based on the interrelation analysis of a high number of process variables [16].

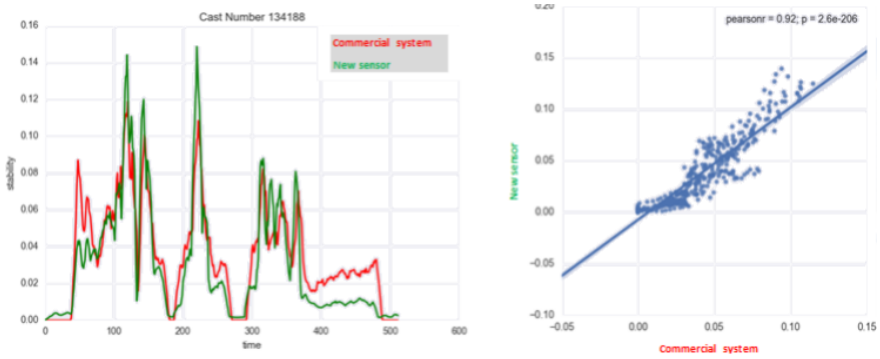

Fig. 7. Direct comparison and linear fitting analysis of stability index of an AMIGE system (red) and by the new proposed sensor (green)

The average Pearson correlation coefficient between the new sensor estimated stability factor index and the one provided by AMIGEsystem[33] was 0.84 with a standard deviation of 0.05 proving that the proposed methodology is able to give same accuracy as consolidated and much more expensive systems. Prices of commercially available systems exceeds 100k€ in all cases, while the implementation cost of the proposed technology is lower than 1k€ requiring no installation or technical modifications requirements.

C. Correlation with image processing slag control & quality system

Finally, although the initially proposed development sought to cover a lack of technology identified for DC EAFs, a general aim of ArcelorMittal Global R&D is to develop generalized industrial solutions for steelmaking sector. A last validation test was carried out in an AC EAF. To this end, the new sensor for measuring arc instabilities was installed nearby an AC EAF in ArcelorMittal. At this location, an image processing system for slag quality assessment is present. This system continuously monitories the liquid slag stream during the desslagging phase and offers as output a quality index value based on slag flow speed and slag width of the slag stream. The image control tool allows doing a gross approximation of slag flow volume, so that, the system is able to estimate a “slag quality index” based on machine vision techniques. The relationship of the slag visual assessment and the arc stability has been already demonstrated by [18]. During this test, the slag quality index generated by the image processing system was directly compared with the arc stability value provided by the proposed new sensor. Fig. 8 depicts the visual appearance of some slags qualities (in the upper side of the picture) and their corresponding arc stability factor (in the lower side). During the deslagging phase, several slag images and its quality assessments were selected and they were compared with the arc stability value offered by the new sensor , demonstrating that the better is the reported Arc Stability Index, the more stable is the arc in the last stage of the EAF melting process (bad slag qualities leads to worse stability factor).

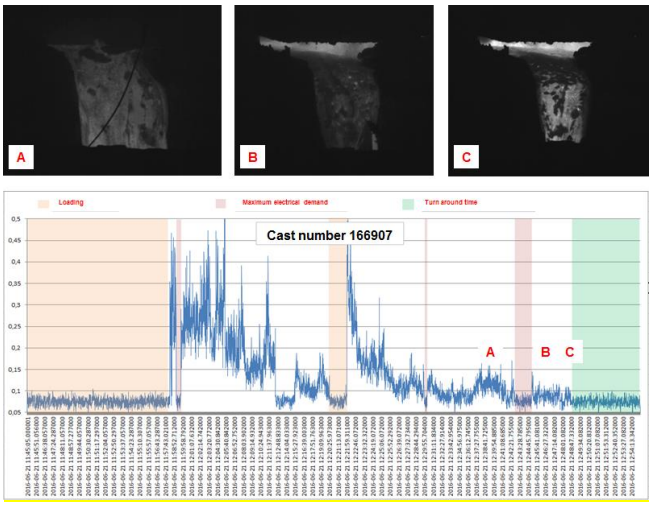

Fig. 8.Top) Visual appearance of different slags: Left) Bad-liquid slag, Middle) Good slag, Right) Good slag. Bottom) Arc stability value. Marks A, B and C represent time stamps when previous slags were recorded

In view of the results of these three validation analyses, it has been proved that the empirical value of the Arc Stability Index by means of a non-intrusive technique, is not only industrially operative, but it also offers high correlation with other type of commercial systems, much more expensive, that are commonly used.

VI. Arc Stability Index Based Closed Loop Regulation

The main objective of developing a new measurement index is to reduce the energy consumption of the EAF process. To this end, an arc stability index based closed loop control has been established. During one-month period, the stability data of all the melts were collected. Spurious castings with specific customer requirements were removed from the analysis. These included start-ups, refractory repairs or heats with excessive TapToTap cycle. Four levels of stability were distinguished (saturation, unstable, stable and Off period). In the initial periods of the melting process, when the furnace contains solid scrap, the arc is very unstable. As the scrap turns into a liquid state and the slag foaming process begins, the level of arc stability increases gradually. Finally, in the last stages of the refining process, as the Iron oxide increases in the slag, the arc becomes unstable.

A. Regulation Algorithm

The new Arc Stability Index is used for reducing the arc voltage (length of the arc) when the instability value exceeds a preset value. For defining the voltage control thresholds, an experienced furnace operator analyzed the furnace behavior regarding the values provided by the ASI for a one-month period. This analysis served for defining V_{1sup} and V_{1inf} as arc totally instable and arc instable respectively (see Fig. 9)
The Arc Stability Index is sent to the EAF electrical regulation PLC in real time and the implemented closed loop control consists on, when the total energy input is higher than 35MWh (to avoid interferences on the initial stages of the process where the scrap is melt), reducing the arc voltage regarding the voltage set point in 60 volts and in 30 volts if the ASI is higher than V_{1sup} and V_{1inf} respectively.

This control system was used to evaluate how the energy consumption of the furnace varies for a given EAF configuration (Scrap mix and O2/C injection models). Based on the predefined thresholds, the process temporal period for the different levels of stability were measured in order to obtain information on the time percentage for stability as it can be seen in Fig. 9. These values will be used for the analysis of the Electric Arc stability index performance.

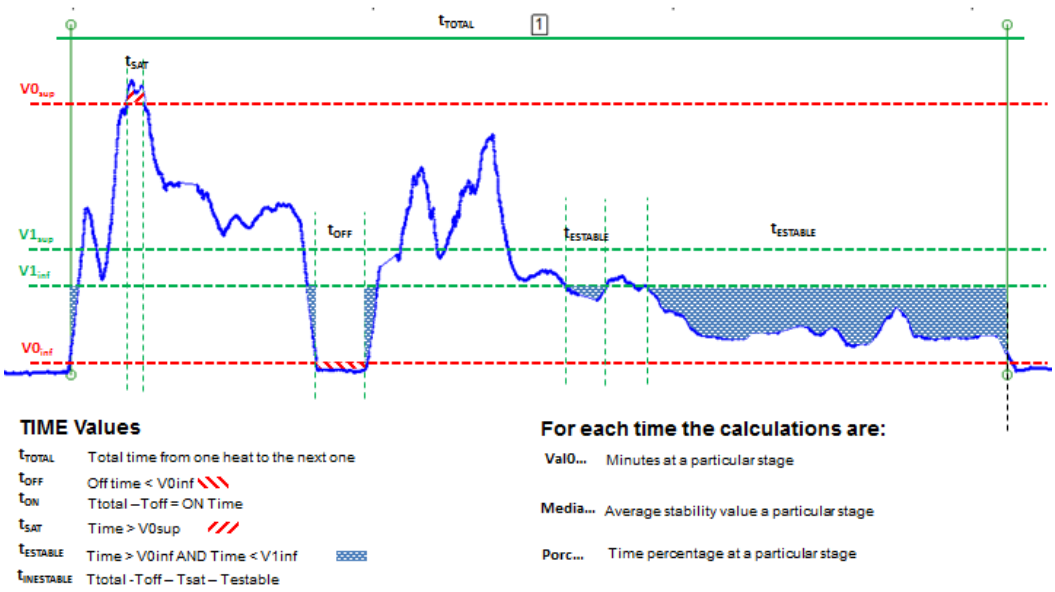

Fig. 9. Mathematical analysis criteria of the stability factor allows to do the analysis only when the furnace is in operation (stability signal between V0 sup and V0 inf), as well as to identify when the energy input is maximized guaranteeing the conditions of stability of the arch (stability signal lower than V1 inf) ,

The new information available (periods time and average stability values in saturation, stable and instable situations), is analyzed on the next section to calculate a model that associates the values of the arc stability index with the power consumption. The methodology proposed in Fig. 10 offers useful information for regulating the voltage level of the arc controller according V1 sup and V1 inf thresholds.

B. Relationship between power consumption and Electric Arc Stability Index

A linear regression function was obtained including information from the different measured stability states: (A= saturation, B= Stable and C= Unstable). From each state, we take the time (minutes) that this stage was active (A_1,B_1,C_1), the average stability value for each stage (A_2, B_2, C_2) and the percentage for each stability stage (A_3, C_3, D_3).

This linear regression function was subsequently evaluated using the melting data for the next month. Fig. 11 shows the results of this analysis. It can be appreciated on the obtained linear regression function that Saturation and Unstable states contribute to a higher power consumption whereas stable states contribute to lower power consumption

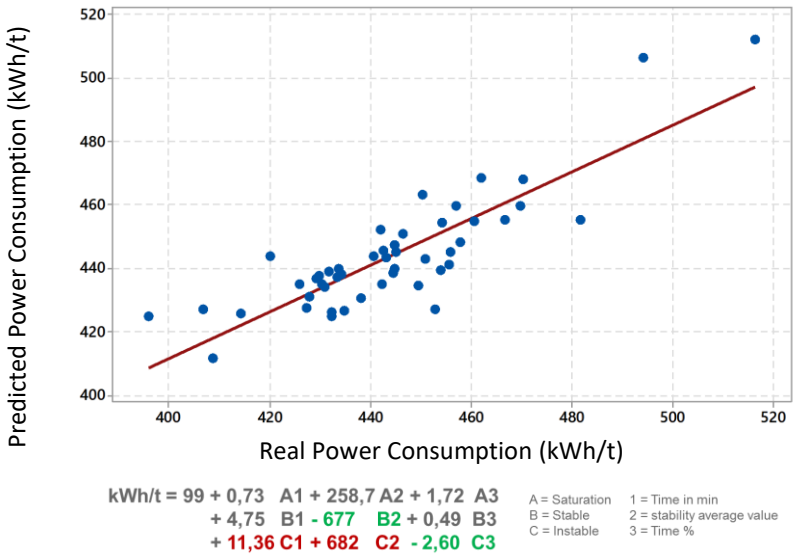

Fig. 11. Prediction of electrical consumption from the stability data

C. Reduction of power consumption based on the arc stability index:

One problem for validating the arc quality index effect on energetic efficiency is related to the high variability on the energetic behavior of the electric arc furnaces. This depends on a large number of process variables that are not easily controlled. These variables are, among others, the heterogeneity of the scrap mix used, the hot heel inside the furnace, the state of the refractory, the state of the carbon and oxygen injectors and the quality of the fluxes used during the melting process.

Because of this, a validation experiment was set where 100 consecutive heats were tested alternatively switching on and off the Arc Stability Index regulation alternating the sensor in on mode and regulating in closed loop the arc voltage (in even referenced heats), with the sensor in off mode (in odd referenced heats) where the voltage control is done following the factory established procedure.

Energy consumption at each cast was recorded showing that the 50 casts following the proposed new arc control methodology led to a reduction of 6.7 kWh per Liquid steel ton during the evaluated period due to an improvement in the electric energy input efficiency to the EAF compared to the 50 casts that did not follow the proposed regulation.

This improvement in efficiency also resulted in a reduction in the power ON time in 1.1 minutes, which significantly increased the productivity of the furnace.

VII. CONCLUSIONS

Currently, there are several commercial systems for monitoring the arc stability in electric arc furnaces in the market. However, most of them are only valid for AC technology and in all the cases the commercial solution requires high CAPEX and an intrusive implementation in the existing automatization.

In this work, we have proposed a new low-cost and non-intrusive 3D sensor for DC electric arc stability control system through the analysis of magnetic field produced around the electrical conductors based on Hall-Effect. This sensor is much cheaper and easier to integrate than current sensors.

We have proposed a new metric for electric arc stability estimation that we called maximum projection based Arc Stability Index. This index has been validated against other measurement methods (acoustic signal, visual assessment and more expensive measurement systems). Besides this, the relationship of the proposed index and energy consumption has been also validated.

The new system was tested in both DC and AC EAFs and industrially integrated with two different DC EAF in ArcelorMittal showing a reduction of 6.7 kWh per Liquid steel ton during the evaluated period and a time reduction of 1.1 minutes per heat.

Arc stability value gives also additional criteria for the most important managerial activities of the Steelshop technicians like evaluating HBI/DRI feeding ratio during the heat, automatic Oxygen / Carbon injection model or fluxes addition strategies. The new available process information opens new research lines in the short and medium term related to energy modeling or environmental footprint reductions not only for steel manufacturing but to other metallurgic processes requiring electric arc furnaces.

REFERENCES

[1] Wu, J. J., Bin, Y. A. N. G., DAI, Y. N., & Morita, K. (2009). Boron removal from metallurgical grade silicon by oxidizing refining. Transactions of Nonferrous Metals Society of China, 19(2), 463-467.

[2] Batra, N. K. (2003). Modelling of ferrosilicon smelting in submerged arc furnaces. Ironmaking & steelmaking, 30(5), 399-404.

[3] A. Vicente, J.A. Gutierrez, J.A. Arteche, I. Macaya. Liquid steel level measurement at EAF without increasing the power off time. 11th European Electric Steelmaking conference & Expo. 2016.

[4] ADAMS, Wayne, et al. Factors influencing the total energy consumption in arc furnaces. En 59 th Electric Furnace Conference and 19 th Process Technology Conference. 2001. p. 691-702.

[5] M. Aula, M. Mäkinen, A. Lepänen, M. Huttula, T. Fabritius. Optical emision analysis of slag surface conditions and furnace atmosphere during different process stages in EAF. ISIJ International 2015. 55 (8) 1702-1710.

[6] C. Di Cecca, A.F. Cluffini, S. Barella, C. Mapelli, A. Gruttadauria, D. Mombelli. Estimation of carbon concentration in the metal bath by means of on-line measurement of the concentration of the off-gas in the EAF. 11th European Electric Steelmaking conference & Expo. 2016.
[7] Picon, A., Vicente, A., Rodriguez-Vaamonde, S., Armentia, J., Arteche, J. A., & Macaya, I. (2017). Ladle furnace slag characterization through hyperspectral reflectance regression model for secondary metallurgy process optimization. IEEE Transactions on Industrial Informatics, 14(8), 3506-3512.
[8] P. Nyssen, C. Mathy, L. Bellavia, M. Weber, J.C. Baumert, M.S. Millman, G. Antonelli. Control by camera of the EAF operation in airtight conditions. EUR 19470 EN. Luxembourg 2010.
[9] "Improved EAF process control using online offgas analysis", Report EUR 25048 EN. RFCS. Luxembourg 2011
[10] M. Plazza, F. Blanco, D. Patrizio, M. Ometto. EAF process optimization through a modular automation system and an adaptive control strategy. 11th European Electric Steelmaking conference & Expo. 2016.
[11] B. Bowman, N. Lugo and T.P. Wells. Influence of tap carbon and arc voltage on electrode and energy consumption. Elec. Furn. Conf. AIME, Orlando, 2000, pp649-57.
[12] B. M. Dehkordi, M. Moallem y A. Parsapour. Predicting Foaming Slag Quality in Electric Arc Furnace Using Power Quality Indices and Fuzzy Method. IEEE Transactions on Instrumentation and Measurement, vol. 60, (2011), pp. 3845 - 3852.
[13] Lavers, J. D., & Biringer, P. P. (1986). Real-time measurement of electric arc-furnace disturbances and parameter variations. IEEE transactions on industry applications, (4), 568-577.
[14] Horton, Randy, Timothy A. Haskew, and Reuben F. Burch IV. "A time-domain ac electric arc furnace model for flicker planning studies." IEEE Transactions On Power Delivery 24.3 (2009): 1450-1457.
[15] Hsu, Yu-Jen, et al. "Electric arc furnace voltage flicker analysis and prediction." IEEE Transactions on Instrumentation and Measurement 60.10 (2011): 3360-3368.
[16] H.B. Lüngen, M.Peters, P.Schmöle. Evolution of EAF technology. AISTech 2012 Proceedings 109-119.
[17] Manchur, G., and C. Cc Erven. "Development of a model for predicting flicker from electric arc furnaces." IEEE Transactions on Power Delivery 7.1 (1992): 416-426.
[18] D. Ameling, J. Petry, M. Sittard, W. Ferich, J. Investigation of foaming slag formation on in the electric arc furnace. Wolf. EISI, 1986, p1-8.
[19] Ramboz, John D. "Machinable Rogowski coil, design, and calibration." IEEE Transactions on Instrumentation and measurement 45.2 (1996): 511-515.
[20] Dehghan Marvasti, Farzad, and Haidar Samet. "Fault detection in the secondary side of electric arc furnace transformer using the primary side data." International Transactions on Electrical Energy Systems 24.10 (2014): 1419-1433.
[21] Eugene B. Pretorius, Robert C. Carlisle. Foamy Slag Fundamentals and their practical application to electric furnace steelmaking. 1998 EAF Conf.
[22] J. Madias, A. Bilancieri, S. Hornby. Global EAF survey:The influence of metallics and EAF design. Steel Times International, Dec 2017.
[23] Martell, Fernando, et al. "Virtual neutral to ground voltage as stability index for electric arc furnaces." ISIJ international 51.11 (2011): 1846-1851.
[24] BOWMAN, Ben B. Arc furnace electrode control. U.S. Patent No 5,115,447, 19 Mayo 1992.
[25] "Evaluation of sound-, current- and vibration measurements in the Electric Arc Furnace", Pär Ljungqvist. Royal Institute of Technology Stockholm, Sweden. 2013
[26] Aula M., Jokinen M., Paavo H., Timo F., Juha R. Why OESmeasurements beats conventional methods in control of EAF. 11th European Electric Arc Furnace Conference (2016) Venice.
[27] Cataliotti, Antonio, et al. "Improvement of Hall effect current transducer metrological performances in the presence of harmonic distortion." IEEE Transactions on Instrumentation and Measurement 59.5 (2010): 1091-1097.
[28] Ripka, Pavel. "Electric current sensors: a review." Measurement Science and Technology 21.11 (2010): 112001.
[29] Tsai, Yuan-Pin, et al. "Multifunctional coreless Hall-effect current transformer for the protection and measurement of power systems." IEEE Transactions on Instrumentation and Measurement 63.3 (2014): 557-565.
[30] Cardoso, AJ Marques, et al. "Rotor cage fault diagnosis in three-phase induction motors, by Park's vector approach." IAS'95. Conference Record of the 1995 IEEE Industry Applications Conference Thirtieth IAS Annual Meeting. Vol. 1. IEEE, 1995.
[31] Ramos, Helena G., and A. Lopes Ribeiro. "Present and future impact of magnetic sensors in NDE." Procedia Engineering 86 (2014): 406-419.
[32] Hwang, C. S., F. Y. Lin, and P. K. Tseng. "A PC-based real-time Hall probe automatic measurement system for magnetic fields [of SRRC magnets]." IEEE Transactions on Instrumentation and Measurement 48.4 (1999): 858-863.
[33] G. Fernandez, F. Samimi, N. Oki, Results In EAF Process Optimization With AMIGE SmartFurnace System, AISTech (2017)
[34] D'Antona, Gabriele, et al. "Processing magnetic sensor array data for AC current measurement in multiconductor systems." IEEE Transactions on Instrumentation and Measurement 50.5 (2001): 1289-1295.